Journal of
Materials Chemistry

Cite this: *J. Mater. Chem.*, 2012, **22**, 2894

www.rsc.org/materials

PAPER

Simple CBP isomers with high triplet energies for highly efficient blue electrophosphorescence†

Shaolong Gong,[a] Xun He,[a] Yonghua Chen,[b] Zuoquan Jiang,[a] Cheng Zhong,[a] Dongge Ma,*[b] Jingui Qin[a] and Chuluo Yang*[a]

Received 30th September 2011, Accepted 8th November 2011
DOI: 10.1039/c1jm14903b

Two simple CBP isomers, namely ***m*-CBP** and ***o*-CBP**, were designed and synthesized by finely tuning the linking topology between the carbazole and the central biphenyl units of **CBP**, and their thermal, photophysical and electrochemical properties were investigated. Such simple modification of the linking topology endows the CBP isomers with high triplet energy and relative high thermal and morphological stability. The high triplet energies of ***m*-CBP** and ***o*-CBP** ensure efficient energy transfer from the host to the phosphor and triplet exciton confinement on the phosphor, as indicated by the transient photoluminescence decay of 3 wt% FIrpic doped into ***m*-CBP** and ***o*-CBP**. Blue phosphorescent devices employing FIrpic as guest and the two CBP isomers as hosts exhibit high efficiencies. The best EL performance is achieved for the ***o*-CBP**-based device, with a maximum current efficiency of 29.9 cd A^{-1}, and a maximum external quantum efficiency of 14.2%, which are over 2 times higher than those of **CBP**.

Introduction

Phosphorescent organic light-emitting diodes (PhOLEDs) have attracted intense interest because of their merit of high quantum efficiency as compared to conventional fluorescent OLEDs through utilizing both singlet and triplet exitons for emission.[1–5] To avoid concentration quenching and triplet–triplet annihilation,[6] phosphorescent emitters of heavy-metal complexes are usually doped into a suitable host material. Therefore, the design and synthesis of host materials are vital to the realization of efficient PhOLEDs.[7] It is desirable that a host material should have high enough triplet energy to suppress triplet energy back transfer from the guest to the host and confine the triplet exciton on the guest molecule.[8] Recently, green and red PhOLEDs with 100% internal quantum efficiency have been reported,[9–12] but highly efficient and stable blue PhOLEDs remain to be developed because of the lack of suitable host materials possessing higher triplet energy levels than blue phosphors.

The carbazole-based compound *N*,*N*′-dicarbazolyl-4,4′-biphenyl (**CBP**) has been widely utilized as the host material for efficient green and red PhOLEDs,[13,14] but it is not an efficient host for blue PhOLEDs because of its lower triplet energy (2.56 eV) relative to that of blue phosphor iridium(III) bis(4,6-(difluorophenyl)pyridine-*N*,$C^{2'}$) picolinate (FIrpic, 2.65 eV).[8] To address the issue, a series of structurally modified CBP-derivatives have been developed. Through replacing the biphenyl unit by a single benzene group in combination with *meta*-position instead of *para*-position between the 9-position of carbazole and phenyl ring, *N*,*N*′-dicarbazolyl-3,5-benzene (*m*CP) with a high triplet energy of 2.9 eV has been reported as host material for blue PhOLEDs.[8] However, problems still remain in terms of relative low thermal and morphological stability due to the decreased molecular weight.[15] Another strategy to increase the triplet energies of CBP-based materials is to incorporate steric group or non-conjugated linkage between the two carbazole moieties. For example, 4,4′-bis(9-carbazolyl)-2,2′-dimethyl-biphenyl (CDBP, 3.0 eV) with two methyl substitution in the 2- and 2′-position of the biphenl unit,[16] and bis(4-(9-carbazolyl)phenyl)diphenylsilane (CPSiCBP, 3.0 eV) with the tetraphenylsilane group as the linkage have been prepared to realize efficient blue electrophosphorescence.[17] Although these materials have high enough triplet energies to host the blue phosphor FIrpic, their complicated multi-step synthesis and moderate to low yields will increase the overall cost of the practical devices. In this study, we designed and synthesized two CBP isomers by finely tuning the linking topology between the two carbazole units and the biphenyl group from

---

[a] *Department of Chemistry, Hubei Key Lab on Organic and Polymeric Optoelectronic Materials, Wuhan University, Wuhan, 430072, People's Republic of China. E-mail: clyang@whu.edu.cn*
[b] *State Key Laboratory of Polymer Physics and Chemistry, Changchun Institute of Applied Chemistry, Chinese Academy of Sciences, Changchun, 130022, People's Republic of China. E-mail: mdg1014@ciac.jl.cn*

† Electronic supplementary information (ESI) available: Crystal data of ***o*-CBP**, TGA traces of ***m*-CBP** and ***o*-CBP**, and UV-vis absorption of **CBP**, ***m*-CBP** and ***o*-CBP** in film state. CCDC reference number 846417. For ESI and crystallographic data in CIF or other electronic format see DOI: 10.1039/c1jm14903b

di-*para*-position to di-*meta*- or di-*ortho*-positions. We anticipate that the simple modification of linking topology would endow the material with relative high triplet energies. We will present a comprehensive investigation that encompasses the thermal, photophysical, and electrochemical properties of the compounds, and demonstrate the applicability of these materials as hosts for blue PhOLEDs.

Experimental

General information

^{1}H NMR and ^{13}C NMR spectra were measured on a MERCURY-VX300 spectrometer. Elemental analyses of carbon, hydrogen, and nitrogen were performed on a Vario EL III microanalyzer. GC-Mass spectra were measured on a Thermo Trace DSQ II GC-MS. UV-Vis absorption spectra were recorded on a Shimadzu UV-2500 recording spectrophotometer. Photoluminescence (PL) spectra were recorded on a Hitachi F-4500 fluorescence spectrophotometer. The PL lifetimes were measured by a single photon counting spectrometer from Edinburgh Instruments (FLS920) with a hydrogen-filled pulse lamp as the excitation source. The data were analyzed by iterative convolution of the luminescence decay profile with the instrument response function using the software package provided by Edinburgh Instruments. Differential scanning calorimetry (DSC) was performed on a NETZSCH DSC 200 PC unit at a heating rate of 10 °C min^{-1} from 20 to 300 °C under argon. The glass transition temperature (T_g) was determined from the second heating scan. Thermogravimetric analysis (TGA) was undertaken with a NETZSCH STA 449C instrument. The thermal stability of the samples under a nitrogen atmosphere was determined by measuring their weight loss while heating at a rate of 10 °C min^{-1} from 25 to 600 °C. Cyclic voltammetry (CV) was carried out in nitrogen-purged dichloromethane (oxidation scan) at room temperature with a CHI voltammetric analyzer. Tetrabutylammonium hexafluorophosphate (TBAPF$_6$) (0.1 M) was used as the supporting electrolyte. The conventional three-electrode configuration consists of a platinum working electrode, a platinum wire auxiliary electrode, and an Ag wire pseudo-reference electrode with ferrocenium-ferrocene (Fc$^+$/Fc) as the internal standard. Cyclic voltammograms were obtained at a scan rate of 100 mV s^{-1}. The onset potential was determined from the intersection of two tangents drawn at the rising and background current of the cyclic voltammogram.

X-Ray structural analysis

Single-crystal X-ray-diffraction data were obtained using a Bruker SMART CCD area-detector diffractometer. The measurements were performed at 292 K using graphite-monochromated Mo-Kα radiation (λ = 0.71073 Å). The data were corrected for absorption using the Siemens area detector absorption (SADABS) program. The structures were solved by direct methods using the SHELXS-97 program. Non-hydrogen atoms were refined with anisotropic thermal parameters by full-matrix least-squares calculations on F^2 using SHELXL-97. Drawings were produced using Diamond 3.0 and Mercury 1.4.1 software. CCDC 846417 (***o*-CBP**) contains supplementary crystallographic data. These data can be obtained free of charge from the Cambridge Crystallographic Data Centre *via* www.ccdc.cam.ac.uk/data_request/cif.

Computational details

The geometrical and electronic properties were performed with the Gaussian 09 program package.[18] The calculation was optimized by means of the B3LYP (Becke three parameters hybrid functional with Lee-Yang-Perdew correlation functionals) with the 6-31G(d) atomic basis set.[19,20] Then the triplet states ΔE (T$_1$–S$_0$) were calculated using time-dependent density functional theory (TD-DFT) calculations with B3LYP/6-311+g(d).

Device fabrication and measurement

The hole-transporting material 1,4-bis[(1-naphthylphenyl)amino]biphenyl (NPB), and electron-transporting material 3-(4-biphenyl)-4-phenyl-5-(4-*tert*-butylphenyl)-1,2,4-triazole (TAZ) were commercially available. Commercial ITO (indium tin oxide) coated glass with sheet resistance of 10 Ω per square was used as the starting substrates. Before device fabrication, the ITO glass substrates were pre-cleaned carefully and treated by oxygen plasma for 2 min. Then the sample was transferred to the deposition system. NPB (80 nm) was firstly deposited to ITO substrate, followed by emissive layer (20 nm), and TAZ (40 nm). Finally, a cathode composed of lithium fluoride (1 nm) and aluminium (100 nm) was sequentially deposited onto the substrate in a vacuum of 10^{-6} Torr. The *J*–*V*–*L* of the devices was measured with a Keithley 2400 Source meter and a Keithley 2000 Source multimeter equipped with a calibrated silicon photodiode. The EL spectra were measured by JY SPEX CCD3000 spectrometer. The EQE values were calculated according to previously reported methods.[21] All measurements were carried out at room temperature under ambient conditions.

Synthesis of materials

9-(3-Bromophenyl)-9*H*-carbazole, 9-[3-(4,4,5,5-tetramethyl-1,3,2-dioxaborolan-2-yl)phenyl]-9*H*-carbazole, 9-(2-bromophenyl)-9*H*-carbazole, 9-[2-(4,4,5,5-tetramethyl-1,3,2-dioxaborolan-2-yl)phenyl]-9*H*-carbazole were prepared according to the reported procedures.[22]

9,9′-Biphenyl-3,3′-diylbis-9*H*-carbazole (*m*-CBP). Dry THF (30 mL) was added to a mixture of 9-(3-bromophenyl)-9*H*-carbazole (0.97 g, 3.00 mmol), 9-[3-(4,4,5,5-tetramethyl-1,3,2-dioxaborolan-2-yl)phenyl]-9*H*-carbazole (1.47 g, 4.00 mmol), K_2CO_3 (2 M in H_2O, 6.0 mL, 12.0 mmol), and $Pd(PPh_3)_4$ (0.069 g, 0.06 mmol). The mixture was refluxed for 48 h under argon. After cooling to room temperature, the mixture was poured into water and extracted with CH_2Cl_2. The organic extracts were collected and dried with anhydrous Na_2SO_4. After removal of the solvent, the residue was purified by column chromatography on silica gel using $CHCl_3$/petroleum (1 : 3 v/v) for the eluent to give ***m*-CBP** as a white powder. Yield: 80%. ^{1}H NMR (300 MHz, $CDCl_3$) δ [ppm]: 8.15 (d, J = 7.8 Hz, 4H), 7.86 (s, 2H), 7.74–7.67 (m, 4H), 7.59 (d, J = 6.9 Hz, 2H), 7.49–7.39 (m, 8H), 7.32–7.25 (m, 4H). ^{13}C NMR (75 MHz, $CDCl_3$) δ [ppm]: 141.34, 140.03, 137.62, 130.00, 125.60, 125.48, 124.87, 122.62, 119.69, 119.46, 109.11. MS (EI): *m*/*z* 484.2 (M$^+$). Anal. calcd for

$C_{36}H_{24}N_2$ (%): C 89.23, H 4.99, N 5.78; found: C 89.53, H 4.64, N 5.64.

9,9′-Biphenyl-2,2′-diylbis-9*H*-carbazole (*o*-CBP). Prepared as a white solid according to a similar procedure to ***m*-CBP**, from 9-(2-bromophenyl)-9*H*-carbazole and 9-[2-(4,4,5,5-tetramethyl-1,3,2-dioxaborolan-2-yl)phenyl]-9*H*-carbazole. Yield: 49%. ^{1}H NMR (300 MHz, $CDCl_3$) δ [ppm]: 7.87 (d, $J = 7.8$ Hz, 4H), 7.72 (d, $J = 6.0$ Hz, 4H), 7.52–7.47 (m, 4H), 7.31–7.26 (m, 4H), 7.04–6.91 (m, 8H). ^{13}C NMR (75 MHz, $CDCl_3$) δ [ppm]: 140.64, 138.14, 136.29, 133.68, 129.22, 129.11, 128.31, 125.24, 123.96, 119.70, 119.60, 110.31. MS (EI): *m/z* 484.3 (M^+). Anal. calcd for $C_{36}H_{24}N_2$ (%): C 89.23, H 4.99, N 5.78; found: C 89.72, H 5.38, N 5.53.

Results and discussion

Synthesis and characterization

The synthetic routes and chemical structures of the CBP isomers, 9,9′-biphenyl-3,3′-diylbis-9*H*-carbazole (***m*-CBP**), and 9,9′-biphenyl-2,2′-diylbis-9*H*-carbazole (***o*-CBP**), are depicted in Scheme 1. The compounds were successfully prepared through Suzuki cross-coupling reactions of the bromide precursors with the corresponding boronic esters.[23] Detailed synthetic procedures are presented in the Experimental section. The chemical structures of both compounds were fully characterized by ^{1}H NMR and ^{13}C NMR, mass spectrometry and elemental analysis. The molecular structure of ***o*-CBP** was further determined by single-crystal X-ray crystallographic analysis, and the crystal data were summarized in Table S1.† As shown in Fig. 1, ***o*-CBP** reveals a twisted molecular structure with a torsion angle of 58.4° between the two phenyl rings of the central biphenyl unit, and torsion angles of 65.5° and 57.8°, respectively, between the two carbazole units and their adjacent phenyl rings. This twist in the structure is beneficial for the reduction of the π-conjugation between the carbazole unit and the central biphenyl group, possibly leading to high triplet energy.[24]

Thermal properties

The thermal properties of the CBP isomers were investigated by thermogravimetric analysis (TGA) and differential scanning calorimetry (DSC). TGA measurement reveals their high thermal-decomposition temperatures (T_d, corresponding to 5% weight loss) of 411 °C (***m*-CBP)** and 317 °C (***o*-CBP**) (Fig. S1).† The DSC trace exhibits distinct glass-transition temperatures (T_g) of 97 °C (***m*-CBP)** and 82 °C (***o*-CBP**) during the second heating scans (Fig. 2), which are significantly higher than 62 °C of **CBP**.[25] In addition, further heating above T_g results in the appearance of crystallisation temperatures (T_c) of 127 °C (***m*-CBP**) and 117 °C (***o*-CBP**) followed by melting peaks of 270 °C (***m*-CBP)** and 248 °C (***o*-CBP**), respectively.

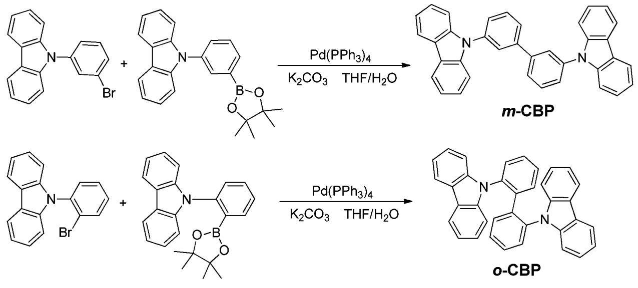

Scheme 1 Synthesis and molecular structures of ***m*-CBP** and ***o*-CBP**.

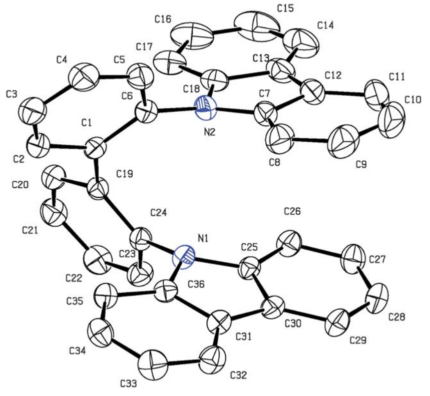

Fig. 1 ORTEP diagram of ***o*-CBP**.

Photophysical properties

Fig. 3 shows the electronic absorption and fluorescence spectra of the CBP isomers. The absorption peak around 293 nm can be assigned to the carbazole-centered π–π* transitions, whereas the absorptions in the range of 319–340 nm could be attributed to π–π* transitions between the carbazole unit and the central biphenyl unit in the molecule. The assignment can be manifested by the fact that the intensity of π–π* transitions for ***m*-CBP** and ***o*-CBP** are remarkably reduced in comparison with the dominant π–π* transition for **CBP**, which could be ascribed to the decreased π-conjugation for ***m*-CBP** and ***o*-CBP** owing to the simple modification of the linking topology.

All compounds show near-ultraviolet emissions between 349–379 nm in dilute toluene solution. Their phosphorescence spectra were measured in a frozen 2-methyltetrahydrofuran matrix at 77 K (Fig. 4), and the triplet energy levels estimated from the highest-energy vibronic sub-band of the phosphorescence spectra follow the sequence of ***o*-CBP** (3.00 eV) > ***m*-CBP** (2.84 eV) >

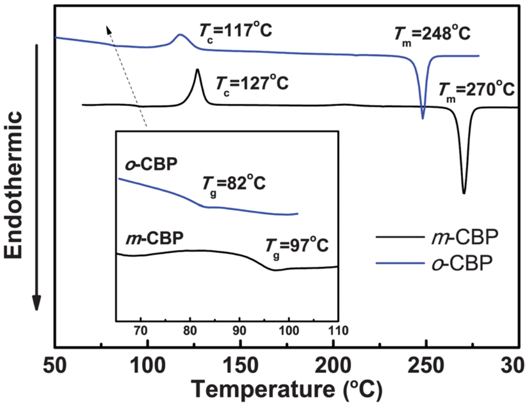

Fig. 2 DSC traces of ***m*-CBP** and ***o*-CBP** recorded at a heating rate of 10 °C min^{-1}.

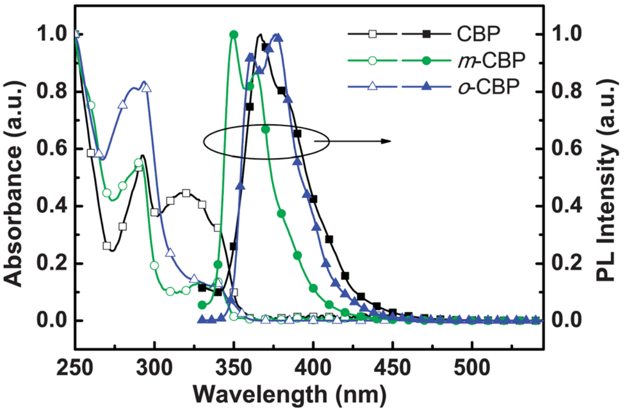

Fig. 3 UV-vis absorption and PL spectra of **CBP**, ***m*-CBP** and ***o*-CBP** in toluene solution at 5 × 10^{-6} M.

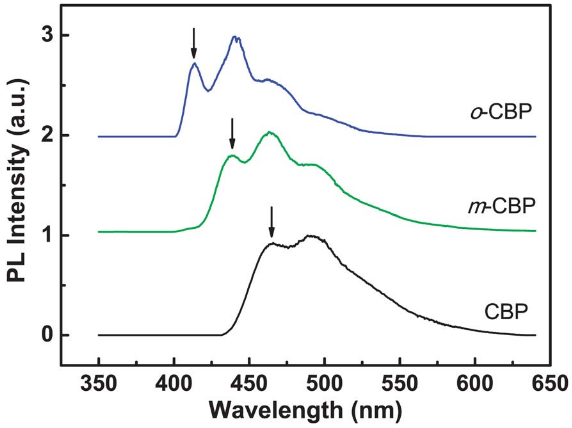

Fig. 4 Phosphorescence spectra of **CBP**, ***m*-CBP** and ***o*-CBP** in a frozen 2-methyltetrahydrofuran matrix at 77 K.

CBP (2.66 eV), which is consistent with the DFT calculated energy order (3.07 > 2.92 > 2.77 eV). Apparently, the π-conjugation between the carbazole and the central biphenyl units for ***m*-CBP** and ***o*-CBP** is decreased by incorporating *meta*-linkage or twisted di-*ortho*-position between these units, resulting in higher triplet energy levels. The triplet energy levels of ***m*-CBP** and ***o*-CBP** are significantly higher than that of blue phosphor FIrpic (2.65 eV), which implies that they could serve as host materials for the blue triplet emitter; whereas the triplet energy level of **CBP** is close to that of FIrpic, suggesting the possible triplet energy back transfer from FIrpic to **CBP** in the device.

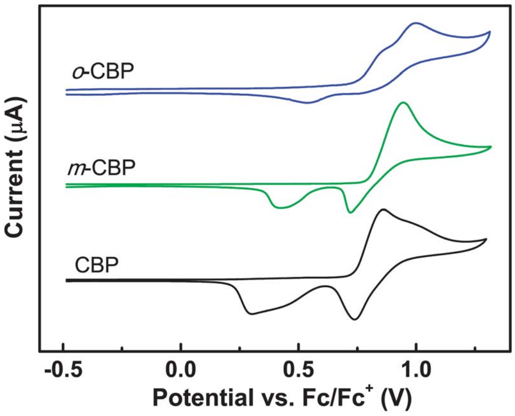

Fig. 5 Cyclic voltammograms of **CBP**, ***m*-CBP** and ***o*-CBP** in CH_2Cl_2 for oxidation.

Electrochemical properties

Cyclic voltammetry (CV) were performed to investigate the electrochemical properties of the compounds (Fig. 5). The two compouds exhibit irreversible oxidation waves like most carbazole derivatives due to the instability of their radical cations.[26] The HOMO energy levels of the compounds were determined from the onset of the oxidation potentials with regard to the energy level of ferrocene (4.8 eV below vacuum). The estimated HOMO levels of ***m*-CBP** and ***o*-CBP** are 5.60 and 5.55 eV, which are similar to that of **CBP** (5.54 eV). Because no clear reduction wave was observed within the potential window of the cyclic voltammograms, the LUMO energy levels were deduced from HOMO energy levels and optical band gaps determined by the onset of absorption (Fig. S2† and Table 1). The deduced LUMO levels are 2.23, 2.13 and 2.19 eV for **CBP**, ***m*-CBP**, and ***o*-CBP**, respectively.

Phosphorescent OLEDs

To evaluate the utility of the two compounds as host materials for blue phosphor FIrpic, we fabricated blue devices by employing the newly designed CBP isomers as the hosts with the configurations of ITO/NPB (80 nm)/hosts: FIrpic (8%, 20 nm)/TAZ (40 nm)/LiF (1 nm)/Al (100 nm). NPB and TAZ were used as the hole- and electron-transporting layers, respectively; LiF served as electron-injecting layer; FIrpic doped in CBP isomers was used as the emitting layer, respectively. For comparison, we also fabricated the control device employing **CBP** as the host. Fig. 6 shows the current density-voltage-brightness (*J*–*V*–*L*) characteristics and efficiency *versus* current density curves for the devices, and the electroluminescence (EL) data are summarized in Table 2. The turn-on voltage of ***m*-CBP** (4.3 V) is higher than those of the devices hosted by **CBP** (3.9 V) and ***o*-CBP** (3.7 V), which is attributed to the lower HOMO level of ***m*-CBP** (5.60 eV) relative to **CBP** (5.54 eV) and ***o*-CBP** (5.55 eV), leading to a large hole-injection barrier (0.2 eV) from the hole-transport NPB layer

Table 1 Physical data of **CBP**, ***m*-CBP** and ***o*-CBP**

	CBP	*m*-CBP	*o*-CBP
$T_g{}^a/T_m/T_d/°C$	62^a/NA/NA	97/270/411	82/248/317
$\lambda_{abs}{}^b$/nm	293/319	292/328	293/340
$\lambda_{em,\ max}{}^b$/nm	366/379	349/363	361/376
HOMO/LUMO^c/eV	5.54/2.23	5.60/2.13	5.55/2.19
$E_{T,\ exp}{}^d$/eV	2.66	2.84	3.00
$\Delta E\ (T_1–S_0)_{cal}{}^e$/eV	2.77	2.92	3.07

[a] The glass-transition temperature was obtained from ref. 25. [b] Measured in toluene. [c] Estimated from the onset of oxidation potentials and the optical band gap from the absorption spectra. [d] Measured in 2-methyltetrahydrofuran matrix at 77 K. [e] Obtained from DFT calculation.

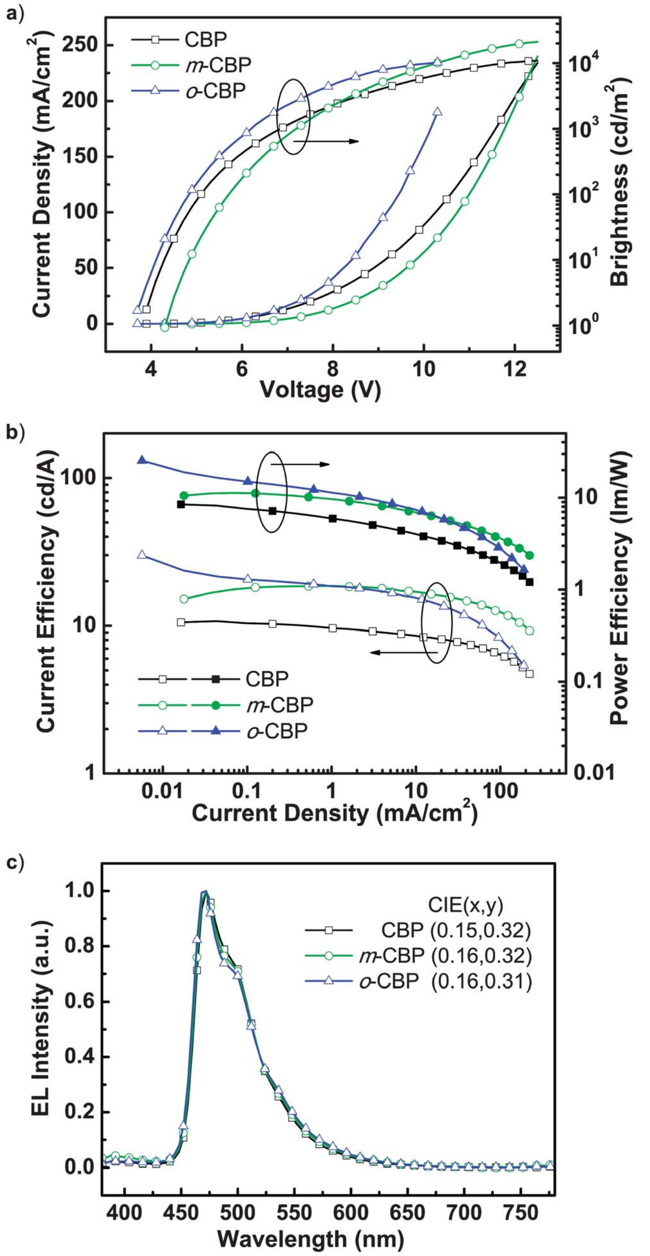

Fig. 6 (a) Current density-voltage-brightness characteristics, (b) current efficiency and power efficiency *versus* current density curves, and (c) EL spectra of blue PhOLEDs with different hosts.

(∼5.4 eV) to the emitting layer.[27] The ***m*-CBP**-based device achieves a maximum current efficiency ($\eta_{c.max}$) of 18.6 cd A^{-1}, a maximum power efficiency ($\eta_{p.max}$) of 11.3 lm W^{-1}, and a maximum external quantum efficiency ($\eta_{ext.max}$) of 8.7%, which are significantly higher than those for **CBP** (10.7 cd A^{-1}, 8.5 lm W^{-1}, 5.2%). This can be attributed to the higher triplet energy level of ***m*-CBP** compared with **CBP**, efficiently suppressing triplet energy back tranfer from the guest to the host. The best EL performance was achieved for the ***o*-CBP**-based device, with $\eta_{c.max}$ of 29.9 cd A^{-1}, $\eta_{p.max}$ of 25.3 lm W^{-1}, and $\eta_{ext.max}$ of 14.2%, which are over 2 times higher than those of **CBP**. This drastic improvement can be rationalized by both its high triplet energy (3.00 eV) ensuring efficient energy transfer from the host to the phosphor and triplet exciton confinement on the phosphor, and its matched HOMO level (5.55 eV) facilitating efficient hole injection to the emitting layer. The EL spectra and the Commission International de I'Eclairage (CIE) coordinates of devices hosted by CBP isomers are shown in Fig. 6c. All devices show the same main peak at 475 nm with a shoulder peak at 500 nm, arising from the typical emittion of the phosphor FIrpic.[28]

To further confirm the triplet exciton confinement properties of CBP isomers and understand the different device performance, we have measured the transient photoluminescence decay of 3 wt% FIrpic doped into **CBP**, ***m*-CBP** and ***o*-CBP**. As shown in Fig. 7, the **CBP**:FIrpic film exhibits a complicated

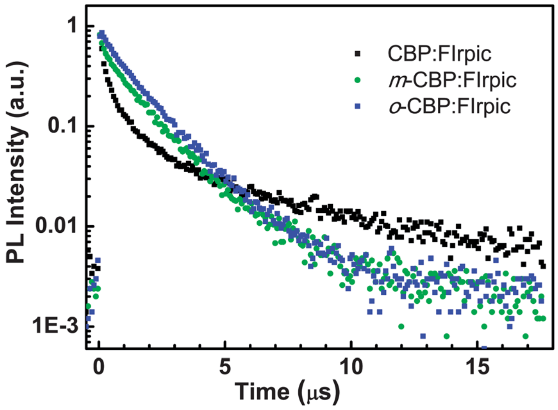

Fig. 7 Decay of the PL intensity (excited at 330 nm) at room temperature at 475 nm from thin films of **CBP**:3 wt% FIrpic, ***m*-CBP**:3 wt% FIrpic, and ***o*-CBP**:3 wt% FIrpic.

Table 2 Electroluminescence characteristics of the devices.[a]

Host	V_{on}[b]/V	L_{max}[c]/cd m^{-2}, Voltages/V	$\eta_{c.max}$[d]/cd A^{-1}	$\eta_{p.max}$[e]/lm W^{-1}	$\eta_{ext.max}$[f] (%)	CIE (x, y)[g]
CBP	3.9	10935 (12.5)	10.7	8.5	5.2	(0.15, 0.32)
***m*-CBP**	4.3	21172 (12.5)	18.6	11.3	8.7	(0.16, 0.32)
***o*-CBP**	3.7	10252 (10.3)	29.9	25.3	14.2	(0.16, 0.31)

[a] Devices configuration: ITO/NPB (80 nm)/EML (20 nm)/TAZ (40 nm)/LiF (1 nm)/Al (100 nm). [b] Turn-on voltages at 1 cd m^{-2}. [c] Maximum luminance. [d] Maximum current efficiency. [e] Maximum power efficiency. [f] Maximum external quantum efficiency. [g] Commission International de I'Eclairage coordinates measured at 7 V.

nonexponential decay curve, indicative of triplet energy back transfer from FIrpic to **CBP**. This can be attributed to the close triplet energy levels of **CBP** (2.66 eV) and FIrpic (2.65 eV), thereby leading to triplet exciton quenching on the **CBP** molecule and then a relatively poor device performance. Both the ***m*-CBP**:FIrpic and ***o*-CBP**:FIrpic films exhibit biexponential decays with relatively long lifetimes of 1.83 and 1.63 μs, respectively. Although these films don't show monoexponential decay curves as expected, their second exponential decay part is far smaller than their first exponential decay component. This can be elucidated from relative high triplet energy levels of 2.84 eV (***m*-CBP**) and 3.00 eV (***o*-CBP**), which successfully suppress triplet energy back transfer from FIrpic to ***m*-CBP** and ***o*-CBP** to confine the triplet exciton on the guest molecule, consequently resulting in efficient blue electrophosphorescence for ***m*-CBP**- and ***o*-CBP**-based devices.

Conclusion

In summary, we have developed two CBP isomers by finely tuning the linking topology between the carbazole unit and the central biphenyl unit from di-*para*-position to di-*meta*- or di-*ortho*-positions. This design strategy endows these materials with high triplet energies, and relative high thermal and morphological stability. We have successfully fabricated highly efficient blue PhOLEDs by employing the simple CBP isomers as host materials. The best EL performance was achieved for the ***o*-CBP**-based device, with $\eta_{\mathrm{c.max}}$ of 29.9 cd A^{-1}, $\eta_{\mathrm{p.max}}$ of 25.3 lm W^{-1}, and $\eta_{\mathrm{ext.max}}$ of 14.2%, which are over 2 times higher than those of **CBP**. This can be attributed to both its high triplet energy (3.00 eV) to confine triplet exciton on the guest and its matched HOMO level (5.55 eV) to facilitate hole injection to the emitting layer. These results demonstrate that simple modification of the linking topology between the carbazole unit and the central biphenyl group of **CBP** is an effective approach to design host materials for highly efficient blue PhOLEDs.

Acknowledgements

The authors thank the National Science Fund for Distinguished Young Scholars of China (No. 51125013), the National Natural Science Foundation of China (No. 90922020), the National Basic Research Program of China (973 Program 2009CB623602 and 2009CB930603), the Fundamental Research Funds for the Central Universities of China, and the Open Research Fund of the State Key Laboratory of Polymer Physics and Chemistry, Changchun Institute of Applied Chemistry, Chinese Academy of Sciences for financial support.

References

1 M. A. Baldo, D. F. O'Brien, Y. You, A. Shoustikov, S. Sibley, M. E. Thompson and S. R. Forrest, *Nature*, 1998, **395**, 151.
2 M. A. Baldo, S. Lamansky, P. E. Burrows, M. E. Thompson and S. R. Forrest, *Appl. Phys. Lett.*, 1999, **75**, 4.
3 A. Köhler, J. Wilson and R. Friend, *Adv. Mater.*, 2002, **14**, 701.
4 P.-I. Shih, C.-H. Chien, C.-Y. Chuang, C.-F. Shu, C.-H. Yang, J.-H. Chen and Y. Chi, *J. Mater. Chem.*, 2007, **17**, 1692.
5 Y.-M. Chen, W.-Y. Hung, H.-W. You, A. Chaskar, H.-C. Ting, H.-F. Chen, K.-T. Wong and Y.-H. Liu, *J. Mater. Chem.*, 2011, **21**, 14971.
6 M. A. Baldo, C. Adachi and S. R. Forrest, *Phys. Rev. B: Condens. Matter*, 2000, **62**, 10967.
7 Y. Tao, C. Yang and J. Qin, *Chem. Soc. Rev.*, 2011, **40**, 2943.
8 R. J. Holmes, S. R. Forrest, Y.-J. Tung, R. C. Kwong, J. J. Brown, S. Garon and M. E. Thompson, *Appl. Phys. Lett.*, 2003, **82**, 2422.
9 H. Sasabe, T. Chiba, S.-J. Su, Y.-J. Pu, K.-I. Nakayama and J. Kido, *Chem. Commun.*, 2008, 5821.
10 Y. Tao, Q. Wang, C. Yang, C. Zhong, K. Zhang, J. Qin and D. Ma, *Adv. Funct. Mater.*, 2010, **20**, 304.
11 C.-H. Chien, F.-M. Hsu, C.-F. Shu and Y. Chi, *Org. Electron.*, 2009, **10**, 871.
12 Y. Tao, Q. Wang, L. Ao, C. Zhong, J. Qin, C. Yang and D. Ma, *J. Mater. Chem.*, 2010, **20**, 1759.
13 C. Adachi, M. A. Baldo, M. E. Thompson and S. R. Forrest, *J. Appl. Phys.*, 2001, **90**, 5048.
14 A. Tsuboyama, H. Iwawaki, M. Furugori, T. Mukaide, J. Kamatani, S. Igawa, T. Moriyama, S. Miura, T. Takiguchi, S. Okada, M. Hoshino and K. Ueno, *J. Am. Chem. Soc.*, 2003, **125**, 12971.
15 Y. Shirota, *J. Mater. Chem.*, 2000, **10**, 1.
16 S. Tokito, T. Ijiima, Y. Suzuri, H. Kita, T. Tsuzuki and F. Sato, *Appl. Phys. Lett.*, 2003, **83**, 569.
17 D. Hu, P. Lu, C. Wang, H. Liu, H. Wang, Z. Wang, T. Fei, X. Gu and Y. Ma, *J. Mater. Chem.*, 2009, **19**, 6143.
18 M. J. Frisch, G. W. Trucks, H. B. Schlegel, G. E. Scuseria, M. A. Robb, J. R. Cheeseman, G. Scalmani, V. Barone, B. Mennucci, G. A. Petersson, H. Nakatsuji, M. Caricato, X. Li, H. P. Hratchian, A. F. Izmaylov, J. Bloino, G. Zheng, J. L. Sonnenberg, M. Hada, M. Ehara, K. Toyota, R. Fukuda, J. Hasegawa, M. Ishida, T. Nakajima, Y. Honda, O. Kitao, H. Nakai, T. Vreven, J. A. Montgomery, Jr., J. E. Peralta, F. Ogliaro, M. Bearpark, J. J. Heyd, E. Brothers, K. N. Kudin, V. N. Staroverov, R. Kobayashi, J. Normand, K. Raghavachari, A. Rendell, J. C. Burant, S. S. Iyengar, J. Tomasi, M. Cossi, N. Rega, J. M. Millam, M. Klene, J. E. Knox, J. B. Cross, V. Bakken, C. Adamo, J. Jaramillo, R. Gomperts, R. E. Stratmann, O. Yazyev, A. J. Austin, R. Cammi, C. Pomelli, J. W. Ochterski, R. L. Martin, K. Morokuma, V. G. Zakrzewski, G. A. Voth, P. Salvador, J. J. Dannenberg, S. Dapprich, A. D. Daniels, O. Farkas, J. B. Foresman, J. V. Ortiz, J. Cioslowski and D. J. Fox, *Gaussian 09 (Revision A.01)*, Gaussian, Inc., Wallingford, CT, 2009.
19 A. D. Becke, *Phys. Rev. A: At., Mol., Opt. Phys.*, 1988, **38**, 3098.
20 C. Lee, W. Yang and R. G. Parr, *Phys. Rev. B*, 1988, **37**, 785.
21 S. R. Forrest, D. D. C. Bradley and M. E. Thompson, *Adv. Mater.*, 2003, **15**, 1043.
22 S.-J. Su, H. Sasabe, T. Takeda and J. Kido, *Chem. Mater.*, 2008, **20**, 1691.
23 N. Miyaura and A. Suzuki, *Chem. Rev.*, 1995, **95**, 2457.
24 Y. Tao, Q. Wang, C. Yang, Q. Wang, Z. Zhang, T. Zou, J. Qin and D. Ma, *Angew. Chem., Int. Ed.*, 2008, **47**, 8104.
25 M.-H. Tsai, Y.-H. Hong, C.-H. Chang, H.-C. Su, C.-C. Wu, A. Matoliukstyte, J. Simokaitiene, S. Grigalevicius, J. V. Grazulevicius and C.-P. Hsu, *Adv. Mater.*, 2007, **19**, 862.
26 G. Zotti, G. Schiavon, S. Zecchin, J.-F. Morin and M. Leclerc, *Macromolecules*, 2002, **35**, 2122.
27 M. E. Kondakova, T. D. Pawlik, R. H. Young, D. J. Giesen, D. Y. Kondakov, C. T. Brown, J. C. Deaton, J. R. Lenhard and K. P. Klubek, *J. Appl. Phys.*, 2008, **104**, 094501.
28 S. Gong, Y. Chen, X. Zhang, P. Cai, C. Zhong, D. Ma, J. Qin and C. Yang, *J. Mater. Chem.*, 2011, **21**, 11197.